Reliable Feedback Generation in Unsynchronized Joint-Processing CoMP Transmission Networks

Stanislaus Iwelski, Erfan Majeed, Zijian Bai, Guido H. Bruck, Peter Jung
Department of Communication Technologies, University of Duisburg-Essen, Germany
E-Mail: {first.surname@kommunikationstechnik.org}

***Abstract*—Coordinated multipoint (CoMP) transmission is a key technique in 4G long term evolution (LTE) systems to provide the ubiquitous broadband communication with cell edge free experience at the user equipment (UE). However, as the transmit signals will reach the UE at several and varying delays, practical CoMP networks might experience large timing offsets (TOs), imposing a significant performance loss. In this paper we focus on implicit feedback generation for practical CoMP joint processing (JP)-joint transmission (JT) networks suffering from TOs. We show that conventional implicit feedback schemes prohibit the expected gain in the downlink, getting outperformed by open-loop transmission schemes and call the benefits of channel state information (CSI) feedback for CoMP JP-JT networks into question. Analytically we prove that the mapping of CSI-reference signal (RS) on different subcarriers imposes multiple phase offsets on the covariance matrix, leading to improper precoding vector selection, while imbalanced TOs among the transmitters limit coherent signal demodulation at the UE. With numerical results we show that estimating and compensating the phase offsets reliable precoding vector selection and phase feedback for coherent signal demodulation can be obtained and as a result considerable improvements for practical CoMP JP-JT networks can be achieved in presence of varying TOs.**

***Index Terms*—Coordinated Multipoint Transmission, LTE-Advanced, Unsynchronized Networks, Timing Offset**

I. Introduction

The 3GPP is continuously enhancing the capabilities of long term evolution (LTE) networks to deal with the irresistible data growth. To provide the ubiquitous broadband access with cell edge free experience [1], next generation technologies including coordinated multipoint (CoMP) transmission are of particular interest to reduce the impact of inter-cell interference [2] and thereby improve the network coverage. Following the concept of CoMP transmission, geographically distributed transmitters are jointly working with conventional or advanced multiple-input and multiple-output (MIMO) schemes [3] to change the cellular network from a interference limited system to a noise limited system [4]. In a typical CoMP scenario the user equipment (UE) is synchronized with the macro base station (BS), also referred to as serving transmission point (TP) and receives data from one or multiple TPs, carried out as remote radio heads (RRHs) [3]. While remarkable system performance gains can be achieved under idealized system conditions [5], practical system implementation suffer from varying timing offsets (TOs) and impair the promised benefits of CoMP transmission in the downlink (DL). The interaction of different propagation delays caused by geographically distributed TPs and different time alignment errors arising from unsynchronized TPs results in the TO [3] and has been identified as the dominant limiting factor from achieving the promised enhancements in practical CoMP transmission [6].

The impact of TO in cooperative systems is investigated from different perspectives in various contributions. In [7] the authors focus on TOs in cooperative MIMO - orthogonal frequency division multiplexing (OFDM) systems, where multiple UEs share the same time-frequency resources to communicate with multiple BSs in the uplink. For simplified system conditions the authors derive a closed-form expression for the signal to interference plus noise ratio and investigate the impact of time arrival differences on the uplink performance analytically. With simulation results the authors generalize their investigation on practical LTE systems, taking their typical OFDM and environmental parameters into account. Cooperative space-time coded OFDM systems with TOs and carrier frequency offsets are investigated in [8], where the authors show that the promised benefits of space-time codes vanish in presence of varying TOs. To maintain the promised advantages of space-time codes the authors suggest to combine this diversity technique with OFDM and time-variant channel estimation.

In our previous works unsynchronized CoMP transmission has been investigated for joint processing (JP)-dynamic point selection (DPS) networks [9]–[11]. While the impact of varying TOs has been generally analyzed in [9], the reason for the performance degradation has been analytically investigated in [10] and, finally a solution has been provided in [11] to maintain the promised advantages of CoMP JP-DPS transmission. In contrast to the previous efforts, in this paper we extend our focus on efficient implicit feedback generation schemes for practical CoMP JP-joint transmission (JT) networks suffering from varying TOs. We show that conventional precoding matrix index (PMI) feedback schemes intended to boost the DL performance in closed-loop transmission impose substantial limitation, fall below the performance of open-loop transmission and therefore question the benefits of feedback generation in CoMP JP-JT networks. We discuss the impact of improper PMI selection in presence of TOs analytically and provide a solution to overcome the limitation. To guarantee the promised advantages of CoMP JP-JT networks in presence of varying TOs we suggest a two-stage implicit feedback generation scheme enabling reliable PMI and phase feedback necessary for proper transmit beamforming and coherent signal demodulation at the UE, respectively. With simulation

978-1-4673-6782-0/15/$31.00 ©2015 IEEE

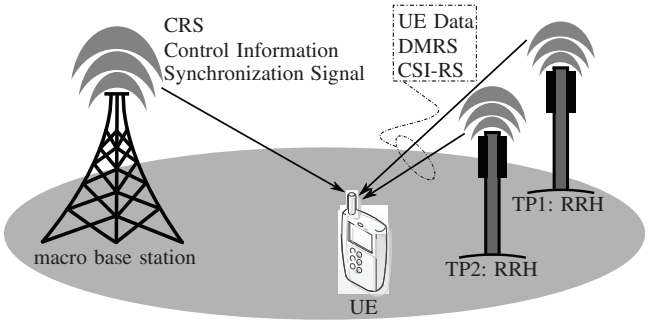

Figure 1. Downlink scenario for CoMP JP-JT network

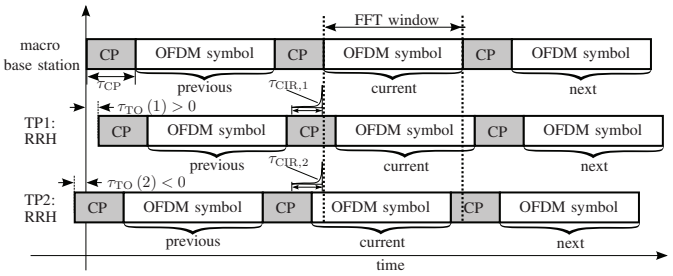

Figure 2. Positive and negative timing offset observed at the UE

results at the link level we discuss the applicability of the suggested two-stage precoder and show that the achievable system performance particularly depends on the estimation quality of the TOs.

The paper is organized as follows: The underlying system model is introduced in Section II. The requirements for reliable implicit feedback generation are presented in Section III with subsequent discussion on simulation results in Section IV. Section V concludes the paper.

II. System Model in CoMP Transmission

A. Cell Layout and Transmission Techniques

CoMP networks provide four different cell layout scenarios in the DL enabling homogeneous and heterogeneous network (HetNet) deployments [3]. While Scenario 1 provides coordination between cells or sectors controlled by the macro BS, Scenario 2 focuses on coordination between cells belonging to different radio sites from the macro network [12]. Beside these homogeneous approaches, two HetNet topologies denotes as Scenario 3 and Scenario 4 enable coordination between the macro BS and low power TPs within the coverage area [12]. The HetNets are of particular interest, as the low power RRHs transmitting data to the UE can be placed inside the macro cell wherever demand for coverage and broadband communication increases. Each of the CoMP scenarios can be set up and operated with either coordination scheduling / coordinated beamforming, transmitter point selection or JP-JT techniques. A comprehensive summary illuminating advantages and practical implementation challenges for the CoMP scenarios and transmission techniques can be found in [12], [13].

To enable broadband communication in poor accessible areas, in this investigation the CoMP JP-JT technique in Scenario 4 is focused on. Scenario 4 is different from all other scenarios, as all TPs within the macro cell share the same cell-ID as the macro BS [3] to keep the data transmission from multiple TPs transparent to the UE. A typical layout for this system configuration is depicted in Figure 1. In this practical DL transmission scheme the UE is synchronized with the macro BS, denoted as TP1, transmitting cell specific reference signal (CRS), control and synchronization signals [14]. The UE data, demodulation reference signals (DMRS) and channel state information (CSI)-reference signal (RS) is typically forwarded via low latency optical fibers to the low power RRHs, denoted as TP1 and TP2 to bring the network closer to the UE.

B. System Function

In the DL scenario with CoMP transmission the UE receives multiple signals from the TPs. The UE evaluates the synchronization signal transmitted by the macro BS and aligns the fast Fourier transform (FFT) window on the currently received OFDM symbol [14], as depicted in Figure 2. As the data signal, the DMRS and the CSI-RS transmitted by the RRHs reach the UE with varying TOs, the FFT window mismatches with the receive signal. To provide an example, the TO is defined as positive with $\tau_{\mathrm{TO}}(1) > 0$, when the transmit signal at the RRH reaches the UE later than the synchronization signal, as depicted in Figure 2 for TP1. On the other hand the TO is defined as negative with $\tau_{\mathrm{TO}}(2) < 0$ if the transmit signal of the RRH arrives prior to the synchronization signal, as depicted in Figure 2 for TP2. To overcome show-stopping negative TOs, it is recommended to relocate the position of the FFT window and turn the negative TO positive [15]. Therefore it is sufficient to concentrate the investigation on positive TOs.

Being synchronized with the macro BS, the receive sum signal $\underline{\boldsymbol{r}}[k] \in \mathbb{C}^{N_{\mathrm{R}}}$ from TP1 and TP2 in the $k-\mathrm{th}$ subcarrier in presence of varying TOs reads

$$
\begin{aligned}
\underline{\boldsymbol{r}}[k] =& \frac{1}{\sqrt{N_{\mathrm{FFT}}}} \sum_{n=1}^{N_{\mathrm{TP}}} \sum_{m=0}^{N_{\mathrm{FFT}}-1} \Bigg(\sum_{\ell=0}^{L-1} \underline{\boldsymbol{H}}_n[m,\ell] \times \\
& \underline{\boldsymbol{e}}_n\left[m + N_{\mathrm{CP}} - \left(\tau_{\mathrm{TO}}(n) + \tau_\ell\right) f_{\mathrm{s}}\right] \Bigg) \times \\
& \exp\left(-\mathrm{j}2\pi \frac{km}{N_{\mathrm{FFT}}}\right) + \underline{\boldsymbol{n}}_{\mathrm{CCI}}[k] + \underline{\boldsymbol{n}}[k] \\
=& \frac{1}{N_{\mathrm{FFT}}} \sum_{n=1}^{N_{\mathrm{TP}}} \sum_{\ell=0}^{L-1} \underline{\boldsymbol{H}}_n[\ell] \exp\left(-\mathrm{j}2\pi \frac{\tau_\ell f_{\mathrm{s}} k}{N_{\mathrm{FFT}}}\right) \times \\
& \sum_{\substack{m=0 \\ k'=0}}^{N_{\mathrm{FFT}}-1} \underline{a}_n[k]\, \underline{\boldsymbol{p}}_n \underline{d}[k] \exp\left(\mathrm{j}2\pi \frac{k'\left(m - \tau_{\mathrm{TO}}(n) f_{\mathrm{s}}\right)}{N_{\mathrm{FFT}}}\right) \times \\
& \exp\left(\mathrm{j}2\pi \frac{km}{N_{\mathrm{FFT}}}\right) + \underbrace{\underline{\boldsymbol{n}}_{\mathrm{I}}[k] + \underline{\boldsymbol{n}}_{\mathrm{CCI}}[k] + \underline{\boldsymbol{n}}[k]}_{\underline{\boldsymbol{n}}_{\sum}[k]}
\end{aligned}
\tag{1}
$$

after OFDM demodulation, where the time domain signal transmitted by the N_{TP} RRHs is denoted by $\underline{\boldsymbol{e}}_n[m] \in \mathbb{C}^{N_{\mathrm{T}}}$, $1 \leq n \leq N_{\mathrm{TP}}$ and $0 \leq m < N_{\mathrm{FFT}} + N_{\mathrm{CP}}$ holds. The FFT size, the length of the cyclic prefix (CP) and the sampling frequency is denoted by N_{FFT}, N_{CP} and f_{s}, respectively. The transmit signal $\underline{\boldsymbol{e}}_n[m]$ is convolved with the time-varying multipath MIMO channel $\underline{\boldsymbol{H}}_n[m,\ell] \in \mathbb{C}^{N_{\mathrm{R}} \times N_{\mathrm{T}}}$, where the time delay variable is denoted by τ_ℓ with a maximum of L taps for all DL channels, while N_{R} and N_{T} denotes the number of receive and transmit antennas, respectively. The channel is assumed to be static over one OFDM symbol with $\underline{\boldsymbol{H}}_n[m,\ell] \approx \underline{\boldsymbol{H}}_n[\ell]$ for $0 \leq m < N_{\mathrm{FFT}} + N_{\mathrm{CP}}$. The precoded transmit symbol in the $k-\mathrm{th}$ subcarrier is defined as $\underline{a}_n[k]\,\underline{\boldsymbol{p}}_n\underline{d}[k]$, where $\underline{a}_n[k] \in \mathbb{C}$ and $\underline{\boldsymbol{p}}_n \in \mathbb{C}^{N_{\mathrm{T}} \times 1}$ represents the complex phase adjustment factor enabling coherent signal demodulation in presence of varying TOs and the precoding vector at the $n-\mathrm{th}$ TP, respectively, while $\underline{d}[k] \in \mathbb{V}$ is the transmit symbol out of the modulation constellation defined by the set $\mathbb{V}$ with $\mathrm{E}\left(\underline{d}[k]\,\underline{d}^*[k]\right) = E_d$. The components of the interference-plus-noise covariance vector $\underline{\boldsymbol{n}}_\Sigma[k]$ are mutually independent, where the co-channel interference vector $\underline{\boldsymbol{n}}_{\mathrm{CCI}}[k] \sim \mathcal{CN}\left(\underline{\mathbf{0}}, \underline{\boldsymbol{R}}_{\mathrm{CCI}}[k]\right)$ represents the interference signal from adjacent transmitters sharing the same resources in the DL. Furthermore the inter-symbol interference (ISI) samples $\underline{\boldsymbol{n}}_{\mathrm{I}}[k]$ are modelled as an additive white gaussian noise (AWGN) component with $\underline{\boldsymbol{n}}_{\mathrm{I}}[k] \sim \mathcal{CN}\left(\underline{\mathbf{0}}, \sigma_{\mathrm{I}}^2\underline{\mathbf{I}}\right)$ and $\underline{\boldsymbol{n}}[k] \sim \mathcal{CN}\left(\underline{\mathbf{0}}, \sigma_n^2\underline{\mathbf{I}}\right)$ holds for the noise vector. Simplifying (1), the MIMO signal representation turns to

$$\underline{\boldsymbol{r}}[k] = \sum_{n=1}^{N_{\mathrm{TP}}} \underline{a}_n[k]\,\underline{\boldsymbol{H}}_n[k]\,\underline{\boldsymbol{p}}_n\underline{d}[k]\,\mathrm{e}^{-\mathrm{j}\phi_n(k)} + \underline{\boldsymbol{n}}_\Sigma[k], \quad (2)$$

where $\phi_n(k) = 2\pi\tau_{\mathrm{TO}}(n)\,f_{\mathrm{s}}k/N_{\mathrm{FFT}}$ represents the phase shift for the particular TO and $\underline{\boldsymbol{H}}_n[k]$ denotes the channel transfer function after OFDM demodulation.

C. Receive Filter Design

To ensure reliable DL transmission in presence of co-channel interference the interference rejection combining (IRC) receiver is selected. This linear receiver is known to provide the best trade-off between interference suppression and receive beamforming, maximizing the post processing signal to noise ratio (SNR) at the receiver. Having knowledge on the interference-plus-noise covariance matrix

$$\underline{\boldsymbol{R}}_\Sigma[k] = \mathrm{E}\left(\underline{\boldsymbol{n}}_\Sigma[k]\,\underline{\boldsymbol{n}}_\Sigma^{\mathrm{H}}[k]\right) = \underline{\boldsymbol{R}}_{\mathrm{CCI}}[k] + \left(\sigma_{\mathrm{I}}^2 + \sigma_n^2\right)\underline{\mathbf{I}} \quad (3)$$

the IRC receiver prewhitens the receive signal using a whitening filter (WF) with a subsequent matched filter (MF) according to

$$\begin{aligned}\underline{\boldsymbol{m}}_{\mathrm{IRC}}^{\mathrm{T}}[k] &= \underbrace{\left(\underline{\boldsymbol{R}}_\Sigma^{-\frac{1}{2}}[k] \times \sum_{n=1}^{N_{\mathrm{TP}}} \underline{\boldsymbol{g}}_n[k]\right)^{\mathrm{H}}}_{\mathrm{MF}} \underbrace{\underline{\boldsymbol{R}}_\Sigma^{-\frac{1}{2}}[k]}_{\mathrm{WF}} \\ &= \left(\sum_{n=1}^{N_{\mathrm{TP}}} \underline{\boldsymbol{g}}_n^{\mathrm{H}}[k]\right)\underline{\boldsymbol{R}}_\Sigma^{-1}[k],\end{aligned} \quad (4)$$

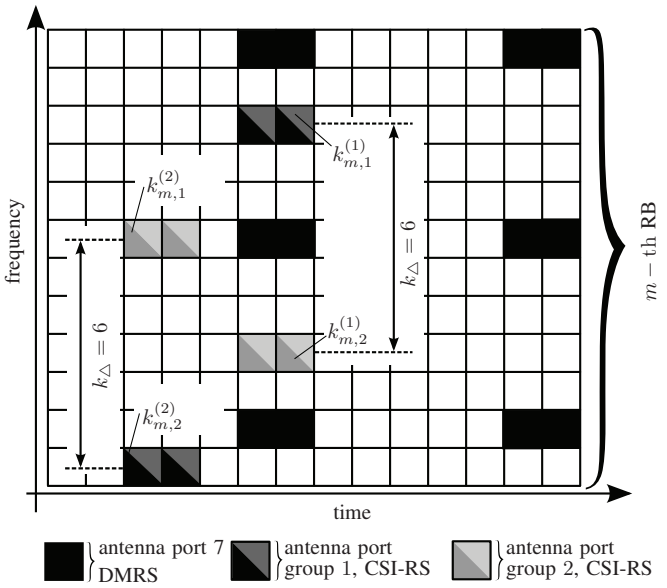

Figure 3. Mapping of reference symbols on resources at TP2

where $\underline{\boldsymbol{g}}_n[k]$ denotes the phase rotated and precoded DL channel for single layer transmission in the $k-\mathrm{th}$ subcarrier with $\underline{\boldsymbol{g}}_n[k] = \underline{a}_n[k]\,\underline{\boldsymbol{H}}_n[k]\,\underline{\boldsymbol{p}}_n\,\mathrm{e}^{-\mathrm{j}\phi_n(k)} \in \mathbb{C}^{N_{\mathrm{R}}}$. Applying the IRC scheme (4) on the receive signal (2) maximizes the post processing SNR $\gamma_{\mathrm{post}}(k)$ according to

$$\gamma_{\mathrm{post}}(k) = E_{\mathrm{d}}\left(\sum_{n=1}^{N_{\mathrm{TP}}} \underline{\boldsymbol{g}}_n^{\mathrm{H}}[k]\right)\underline{\boldsymbol{R}}_\Sigma^{-1}[k]\left(\sum_{n=1}^{N_{\mathrm{TP}}} \underline{\boldsymbol{g}}_n[k]\right). \quad (5)$$

III. Reliable Implicit Feedback Generation in CoMP JP-JT Networks

A. Requirements on Antenna Port Co-Location

Following the requirements for UEs operating in CoMP transmission, is should be possible to send the data signal completely independent from how and where the CRSs is transmitted, as long as the varying TOs are sufficiently covered by the CP [16]. However, to assist and improve DMRS channel estimation, the UE may assume quasi co-location (QCL) w.r.t large scale properties [6] between antenna ports within a resource transmitting DMRS and CSI-RS [17]. In a practical realization of CoMP Scenario 4 this property implicates that the DMRS and CSI-RS transmitted by the $n-\mathrm{th}$ TP suffer from the same TO towards the macro BS the UE is synchronized with. This property is of particular importance, as CoMP JP-JT schemes supporting closed-loop transmission provide remarkable advantages over single cell networks when the feedback information is properly designed [18]. Among the supported feedback schemes the single frequency network (SFN) type 3, also known as multiple single precoding with identical precoding across cells [18] provides the best trade-off between feedback overhead and DL performance [19] and is therefore considered as a practical PMI feedback scheme in this investigation. Following the QCL assumption among the

$$\widehat{\underline{\boldsymbol{R}}}^{\{m\}}(j,i)=\begin{bmatrix}\underline{\Xi}_{1,1}^{\{m\}}(j,i)\,\mathrm{e}^{\mathrm{j}\left(\phi_j\left(k_{m,1}^{(j)}\right)-\phi_i\left(k_{m,1}^{(i)}\right)\right)} & \underline{\Xi}_{1,2}^{\{m\}}(j,i)\,\mathrm{e}^{-\mathrm{j}\left(\phi_j\left(k_{m,1}^{(j)}\right)-\phi_i\left(k_{m,2}^{(i)}\right)\right)}\\ \underline{\Xi}_{2,1}^{\{m\}}(j,i)\,\mathrm{e}^{\mathrm{j}\left(\phi_j\left(k_{m,2}^{(j)}\right)-\phi_i\left(k_{m,1}^{(i)}\right)\right)} & \underline{\Xi}_{2,2}^{\{m\}}(j,i)\,\mathrm{e}^{\mathrm{j}\left(\phi_j\left(k_{m,2}^{(j)}\right)-\phi_i\left(k_{m,2}^{(i)}\right)\right)}\end{bmatrix} \tag{6}$$

antenna ports transmitting DMRS and CSI-RS, the precoding vector maximizing the post-SNR (5) is found by

$$\underline{\boldsymbol{p}}_n=\arg\max_{\underline{\boldsymbol{p}}_i\in\mathcal{S}_{\mathrm{PMI}}}\underline{\boldsymbol{p}}_i^{\mathrm{H}}\underbrace{\sum_{k\in\mathcal{S}_{\mathrm{PRG}}}\underline{\boldsymbol{H}}_{\Sigma}^{\mathrm{H}}[k]\,\underline{\boldsymbol{R}}_{\Sigma}^{-1}[k]\,\underline{\boldsymbol{H}}_{\Sigma}[k]}_{:=\underline{\boldsymbol{R}}_{\mathrm{T}}}\underline{\boldsymbol{p}}_i \tag{7}$$

where $\mathcal{S}_{\mathrm{PMI}}$ denotes the set of candidate precoding vectors [20]. Furthermore, $\underline{\boldsymbol{H}}_{\Sigma}[k]=\sum_{n=1}^{N_{\mathrm{TP}}}\underline{\boldsymbol{H}}_n[k]$ holds for the virtual channel matrix, while $\underline{\boldsymbol{R}}_{\mathrm{T}}$ denotes the maximum likelihood (ML) estimation of the covariance matrix over a finite transmission bandwidth in terms physical resource groups (PRGs) defined by the set $\mathcal{S}_{\mathrm{PRG}}$ [21] in which the selected precoding vector $\underline{\boldsymbol{p}}_n$ remains unchanged.

B. Impact of Timing Offsets on Precoding Vector Selection in SFN type 3 Networks

Accurate channel estimation is necessary to support the transmitter with reliable CSI. In a practical implementation of CoMP JP-JT networks with four transmit antennas at each TP, the CSI-RS are transmitted on two antenna port groups consisting of two antenna ports each [20]. To avoid mutual interference between CSI-RS, different CSI configuration with orthogonal resources can be allocated [3]. Following this recommendation, the $n-\mathrm{th}$ TP allocates the $k_{m,1}^{(n)}-\mathrm{th}$ and $k_{m,2}^{(n)}-\mathrm{th}$ subcarrier to transmit the CSI-RS on the first and second antenna port group in the $m-\mathrm{th}$ resource block (RB), respectively, as depicted in Figure 3. Evaluating the CSI-RS in presence of TO, the estimated channel at the $n-\mathrm{th}$ TP after OFDM demodulation reads

$$\widetilde{\underline{\boldsymbol{H}}}^{(n)\{m\}}=\left[\underline{\boldsymbol{H}}_1^{(n)\{m\}}\mathrm{e}^{-\mathrm{j}\phi_n\left(k_{m,1}^{(n)}\right)},\underline{\boldsymbol{H}}_2^{(n)\{m\}}\mathrm{e}^{-\mathrm{j}\phi_n\left(k_{m,2}^{(n)}\right)}\right]. \tag{8}$$

The sub matrix $\underline{\boldsymbol{H}}_u^{(n)\{m\}}\in\mathbb{C}^{N_{\mathrm{R}}\times 2}$ represents the DL channel between the $u-\mathrm{th}$ antenna port group of the $n-\mathrm{th}$ TP and the N_{R} receive antennas at the UE and reads

$$\underline{\boldsymbol{H}}_u^{(n)\{m\}}=\left[\underline{\boldsymbol{h}}_{1,u}^{(n)\{m\}},\ldots,\underline{\boldsymbol{h}}_{N_{\mathrm{R}},u}^{(n)\{m\}}\right]^{\mathrm{T}}, \tag{9}$$

where $\underline{\boldsymbol{h}}_{\ell,u}^{(n)\{m\}}=\left[\underline{h}_{\ell,15+2(u-1)}^{(n)\{m\}},\underline{h}_{\ell,15+2u-1}^{(n)\{m\}}\right]^{\mathrm{T}}$ holds for $1\leq\ell\leq N_{\mathrm{R}}$ and $1\leq u\leq 2$. Taking the varying TOs into consideration, the ML estimation of the covariance matrix in the PRG for SFN type 3 networks turns to

$$\widehat{\underline{\boldsymbol{R}}}_{\mathrm{PRG}}=\sum_{m\in\mathcal{S}_{\mathrm{PRG}}}\sum_{i=2}^{N_{\mathrm{TP}}}\sum_{j=2}^{N_{\mathrm{TP}}}\underbrace{\widetilde{\underline{\boldsymbol{H}}}^{(i)\{m\}\mathrm{H}}\left(\widehat{\underline{\boldsymbol{R}}}_{\Sigma}^{\{m\}}\right)^{-1}\widetilde{\underline{\boldsymbol{H}}}^{(j)\{m\}}}_{=\widehat{\underline{\boldsymbol{R}}}^{\{m\}}(j,i)}, \tag{10}$$

where $\widehat{\underline{\boldsymbol{R}}}^{\{m\}}(j,i)$ describes the covariance and cross-covariance matrix among the channel matrices for $i=j$ and $i\neq j$, respectively, while $\widehat{\underline{\boldsymbol{R}}}_{\Sigma}^{\{m\}}$ represents the estimation of the interference plus noise covariance matrix in (3) and is defined in equation (10) in [11]. Extending the covariance matrix in [10] for JP-JT networks to consider additionally the cross correction of channel matrices arising in presence of varying TOs, $\widehat{\underline{\boldsymbol{R}}}^{\{m\}}(j,i)$ is explicitly defined in (6) with

$$\underline{\Xi}_{\mu,\lambda}^{\{m\}}(j,i)=\sum_{\ell=1}^{N_{\mathrm{R}}}\sum_{\nu=1}^{N_{\mathrm{R}}}\left(\left(\underline{\boldsymbol{h}}_{\ell,\mu}^{(j)\{m\}}\cdot\left[\underline{\boldsymbol{h}}_{\nu,\lambda}^{(i)\{m\}}\right]^{\mathrm{H}}\right)^{*}\underline{r}'_{\mu,\lambda}\underline{\mathbf{I}}\right), \tag{11}$$

where $\underline{r}'_{\mu,\lambda}$ denotes the $(\mu,\lambda)-\mathrm{th}$ element of the inverse interference plus noise covariance matrix defined in equation (10) in [11]. The estimated covariance matrix in (6) provides information of TO on PMI selection.

Analyzing (6) for the case $i=j=n\in\{1,2\}$ with valid QCL assumption among the antenna ports transmitting DMRS and CSI-RS within the $n-\mathrm{th}$ TP, the phase offset at $\underline{\Xi}_{1,1}^{\{m\}}(n,n)$ and $\underline{\Xi}_{2,2}^{\{m\}}(n,n)$ vanishes due to the balanced phase de-rotation denoted by the $(\cdot)^{\mathrm{H}}$ operation in (11) with subsequent phase rotation. However, the sub-cross covariance matrices $\underline{\Xi}_{1,2}^{\{m\}}(n,n)$ and $\underline{\Xi}_{2,1}^{\{m\}}(n,n)$ are faced by the phase offset $\phi_n\left(k_{m,2}^{(n)}\right)-\phi_n\left(k_{m,1}^{(n)}\right)=2\pi\tau_{\mathrm{TO}}(n)\,f_{\mathrm{s}}k_{\triangle}/N_{\mathrm{FFT}}$ which inherits from imbalanced phase de-rotation and subsequent phase rotation, as the antenna ports transmitting the CSI-RS are located on different subcarriers with spacing $k_{\triangle}=k_{m,2}^{(n)}-k_{m,1}^{(n)}$, as depicted in Figure 3. For $i\neq j$ the covariance matrix in (6) describes the cross correlation between the channel matrices of different TPs where the QCL assumption expires. Despite the previous case, all matrices $\underline{\Xi}_{\mu,\lambda}^{\{m\}}(j,i)$ suffer from a phase offset for $1\leq\mu,\lambda\leq 2$ due to different TOs among the TPs and different subcarriers being allocated to transmit the CSI-RS on the antenna port groups. All these phase offsets impose systematic errors on the ML estimation of the covariance matrix, leading to improper PMI feedback in SFN type 3 networks. In that case the selected PMI does no longer maximize the post-SNR and limits the advantages of closed-loop CoMP JP-JT networks.

C. Two-Stage Implicit Feedback Generation Scheme

To maximize the post-SNR (5), a two-stage implicit feedback generation scheme is suggested, enabling reliable transmit signal precoding in presence of varying TOs. In the first stage the phase offsets affecting the covariance matrix $\widehat{\underline{\boldsymbol{R}}}^{\{m\}}(j,i)$ in (6) for both, $i=j$ and $i\neq j$, $1\leq i,j\leq N_{\mathrm{TP}}$ are compensated to support the RRHs with proper PMI feedback, while in the second stage phase feedback is provided to ensure coherent signal demodulation at the UE operating in practical CoMP JP-JT networks. Both stages are based on accurate TO estimation. As the CSI-RS are mapped on orthogonal resources to avoid mutual interference, the UE is able

Table I
SIMULATION PARAMETERS

Parameter	Value
System Bandwidth / Sampling Rate	10 MHz/15.36MHz
Cyclic Prefix (CP)	4.7 µs
FFT Size / Active Subcarriers	1024/600
Channel Model	SCM-B [22]
Cell Layout	$N_{\mathrm{TP}} = 3$
serving TP	macro eNodeB: TP1
data transmission	RRHs: TP2 and TP3
$N_{\mathrm{T}} \times N_{\mathrm{R}}$	4×2
Implicit Feedback	PMI for SFN type 3
Channel Estimation	Least Square
Receiver	IRC receiver
Transmit configuration	CoMP JP-JT operating in open-loop and closed-loop mode
Timing Offset	$\tau_{\mathrm{TO}}(1)$=1.5 µs, $\tau_{\mathrm{TO}}(2)$=2.5 µs
Timing Offset Estimation	using orthogonal CSI-RS
Interference to Noise Ratio (INR)	10 dB
Modulation	64 QAM

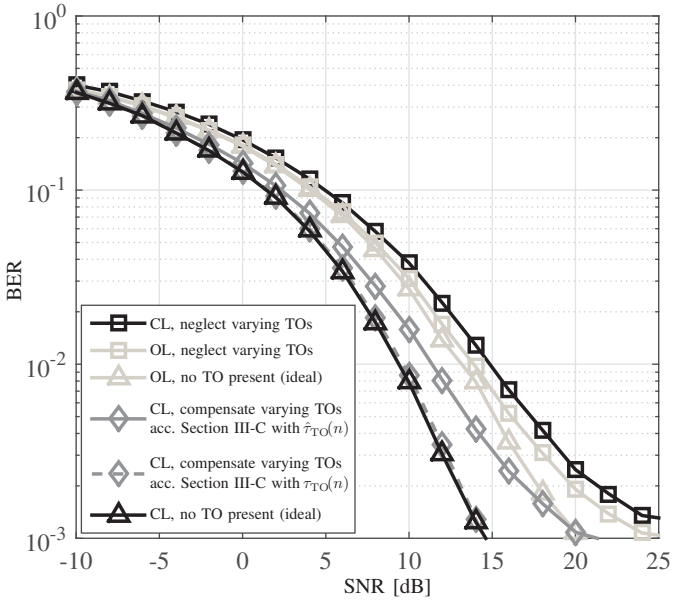

Figure 4. Performance comparison between ideal CoMP JP-JT networks with no TO present ($\tau_{\mathrm{TO}}(1) = \tau_{\mathrm{TO}}(2) = 0\,\mu\mathrm{s}$) and practical system restriction with varying TOs ($\tau_{\mathrm{TO}}(1) = 1.5\,\mu\mathrm{s}, \tau_{\mathrm{TO}}(2) = 2.5\,\mu\mathrm{s}$) for open-loop (OL) and closed-loop (CL) transmission

to estimate the TOs at the RRHs with a theoretical accuracy of $|\hat{\tau}_{\mathrm{TO}}(n)| \leq N_{\mathrm{FFT}}/(2 f_{\mathrm{s}} k_{\delta}) = 2.78\,\mu\mathrm{s}$, where $k_{\delta} = 12$ denotes the subcarrier spacing between the subsequent CSI-RS transmitted by the same antenna port group [20]. Following [15], the TO at each RRH and the associated phase offset can be estimated with $\hat{\phi}_n(k_{m,u}^{(n)}) = 2\pi\hat{\tau}_{\mathrm{TO}}(n) f_{\mathrm{s}} k_{m,k}^{(n)}/N_{\mathrm{FFT}}$ enabling phase offset compensation at the covariance matrix (6) to provide reliable PMI feedback. To enable coherent signal demodulation, the transmit signal at one of the two RRH has to be phase shifted. The phase shift is linearly proportional with the difference of the TOs and is applied on TP2 with $a_2[k] = \exp(\mathrm{j}2\pi f_{\mathrm{s}} k(\hat{\tau}_{\mathrm{TO}}(1) - \hat{\tau}_{\mathrm{TO}}(2))/N_{\mathrm{FFT}})$, while $a_1[k] = 1$ holds.

IV. SIMULATION RESULTS

Simulation results at the link level are carried out to demonstrate the impact of TOs on implicit feedback generation and show the necessity of reliable PMI and phase feedback to maintain the promised advantages of practical closed-loop CoMP JP-JT networks. The assumed system parameters are summarized in Table I, while numerical results are depicted in Figure 4 comparing the performance of ideal and practical system condition for open-loop and closed-loop transmission in the DL. The performance is evaluated at $\mathrm{BER} = 10^{-2}$ unless otherwise stated.

The presence of varying TOs in CoMP JP-JT networks is crucial, limiting the expected DL performance in the closed-loop transmission mode by 5.5 dB when using conventional implicit feedback generation schemes which neglect the TO, as depicted in Figure 4. Following the findings in Section III-B the individual covariance matrices and cross-covariance matrices are affected by individual phase-offsets and impose a systematic error on $\underline{\widehat{\boldsymbol{R}}}_{\mathrm{PRG}}$ after aggregation. Evaluating this corrupted ML estimation of the covariance matrix for precoding vector selection results in improper PMI feedback such that the main lobe of the transmit beam does not reach the UE properly and therefore limits the overall system performance. This limitation is so substantial that the closed-loop transmission scheme intended to assist the transmitters with reliable CSI feedback and thereby boost the DL performance falls 0.9 dB below the performance of open-loop transmission when the TOs are neglected, as depicted in Figure 4. Under these circumstances implicit feedback generation seems totally useless for practical closed-loop CoMP JP-JT networks suffering from varying TOs.

The gap between the two open-loop transmission schemes of 0.7 dB inherits mainly from non-coherent signal reception at the UE, as the imbalanced TOs $\tau_{\mathrm{TO}}(1) \neq \tau_{\mathrm{TO}}(2)$ lead to imbalanced phase offsets after OFDM demodulation. Although the delay span of the channel impulse response with the largest TO exceeds the CP, the main energy of the channel in located in the first taps such that the signals can be considered as sufficiently covered by the CP.

To maintain the promised advantages of closed-loop CoMP JP-JT networks suffering from varying TOs the two-stage implicit feedback generation scheme discussed in Section III-C is utilized. By exploiting the orthogonal resources for CSI-RS transmission the varying TOs can be estimated and, hence the individual phase-offsets affecting the covariance and cross-covariance matrices can be compensated prior to calculate the accumulated ML estimation of the covariance matrix $\underline{\widehat{\boldsymbol{R}}}_{\mathrm{PRG}}$, enabling reliable PMI feedback. On the other hand the transmit signals can be precoded to improve coherence signal reception at the UE. Applying the suggested two-stage implicit feedback

scheme with estimated TOs $\hat{\tau}_{\mathrm{TO}}(n)$ for $n \in \{1,2\}$ the DL performance of practical CoMP JP-JT networks operating in closed-loop mode can be improved by $3.5\,\mathrm{dB}$, as depicted in Figure 4. Further improvements of $1.8\,\mathrm{dB}$ to reach the performance of ideal closed-loop CoMP JP-JT networks is particularly limited by the insufficient estimation accuracy of the TOs caused by the low coherence bandwidth of the frequency selective channel or put another way by the large spacing of the subcarriers carrying the CSI-RS. Applying the two-stage implicit feedback generation scheme with perfect information on the TOs denoted as $\tau_{\mathrm{TO}}(n)$ for $n \in \{1,2\}$, near optimum DL performance can be achieved for practical CoMP JP-JT networks operating in closed-loop mode, as depicted in Figure 4.

V. Conclusion

In this paper the impact of TO on efficient implicit feedback generation for practical CoMP JP-JT networks has been focused on. We have shown that conventional PMI selection schemes prohibit the expected gain in the DL, getting outperformed by open-loop transmission schemes. Two major reasons limiting the expected performance gain have been identified and investigated analytically. The mapping of CSI-RS on different subcarriers on the one hand imposes systematic phase offsets on the estimated covariance matrix, exploited for implicit feedback generation after OFDM demodulation and as a direct consequence leads to improper PMI feedback. On the other hand coherent signal demodulation of the multiple transmit signals is sustainably limited by the TOs among the geometrically distributed RRHs. To overcome these limitations we have suggested a two-stage implicit feedback generation scheme composed of TO estimation and phase offset compensation at the covariance and cross-covariance matrices to guarantee reliable PMI feedback with subsequent phase feedback to enable coherence signal demodulation at the UE. Simulation results prove that applying the suggested two-stage feedback scheme the DL performance of practical CoMP JP-JT systems suffering from varying TOs can be improved considerably, while the achievable gain depends on a great extent on the estimation accuracy of the TOs.

Acknowledgment

The authors wish to gratefully acknowledge the support of their colleagues at Intel Mobile Communications and at the Department of Communication Technologies of University of Duisburg-Essen.

References

[1] Huawei, "The second phase of LTE-Advanced," Huawei, Tech. Rep., 2013.
[2] Erricson, "LTE Release 12," Erricson, Tech. Rep., 01 2013.
[3] 3GPPTSG-RANWG1, "Coordinated Multi-point operation for LTE physical layer aspects," 3GPP, Sophia Antipolis, Technical Report 36.819 v11.2.0, Sep. 2013.
[4] A. Ghosh *et al.*, *Fundamentals of LTE*. Pearson Education Inc., 2011.
[5] Nokia, "Nokia Networks LTE-Advanced," Nokia, Tech. Rep., 09 2014.
[6] Intel Corporation, "Investigation of UE performance degradation due to timing offset between transmission points," 3GPP, New Orleans, USA, Technical Report R4-126255, Nov. 2012.
[7] V. Kotzsch *et al.*, "On timing constraints and OFDM parameter design for cooperating basestations," in *Smart Antennas (WSA), 2010 International ITG Workshop on*, Feb 2010, pp. 169–176.
[8] F. Sanchez *et al.*, "Cooperative Space-Time Coded OFDM with Timing Errors and Carrier Frequency Offsets," in *Communications (ICC), 2011 IEEE International Conference on*, June 2011, pp. 1–5.
[9] S. Iwelski *et al.*, "On the performance of CoMP transmission in unsynchronized networks with timing offset," in *Wireless Communications and Networking Conference (WCNC), 2014 IEEE*, April 2014.
[10] ——, "Feedback Generation for CoMP Transmission in Unsynchronized Networks with Timing Offset," *Communications Letters, IEEE*, 2014.
[11] ——, "Reliable implicit feedback generation in unsynchronized CoMP transmission," in *Personal, Indoor, and Mobile Radio Communication (PIMRC), 2014 IEEE 25th Annual International Symposium on*, Sept 2014.
[12] D. Lee *et al.*, "Coordinated multipoint transmission and reception in LTE-advanced: deployment scenarios and operational challenges," *Communications Magazine, IEEE*, vol. 50, no. 2, pp. 148–155, February 2012.
[13] J. Lee *et al.*, "Coordinated Multipoint Transmission and Reception in LTE-Advanced Systems," *Communications Magazine, IEEE*, vol. 50, no. 11, pp. 44–50, 2012.
[14] Intel Corporation, "Investigation of UE performance degradation due to frequency offset between transmission points," 3GPP, New Orleans, USA, Technical Report R4-126256, Nov. 2012.
[15] S. Iwelski *et al.*, "Robust FFT Window Replacement in Non-Ideal CoMP Networks with Timing Offset," in *Vehicular Technology Conference (VTC Spring), 2014 IEEE 79th*, May 2014, pp. 1–5.
[16] Ericsson, "Geographically separated antennas and impact on CSI estimation," 3GPP, Dresden, Germany, Technical Report R4-120679, Feb. 2012.
[17] ——, "LS response on antenna port co-location," 3GPP, Qingdao, China, Technical Report R1-124020, Aug. 2012.
[18] ETRI, "Per-cell precoding methdos for downlink joint processing CoMP," 3GPP, Prague, Czech Republic, Technical Report R1-083546, Oct. 2008.
[19] Z. Bai *et al.*, "Evaluation of Implicit Feedback in Coordinated Multipoint Transmission beyond LTE-Advanced," in *Vehicular Technology Conference (VTC Spring), 2013 IEEE 77th*, June 2013, pp. 1–5.
[20] 3GPP, "Evolved Universal Terrestrial Radio Access (E-UTRA); Physical Channels and Modulation," 3GPP, Sophia Antipolis, Technical Specification 36.211 v.11.4.0, Sep. 2013.
[21] ——, "Evolved Universal Terrestrial Radio Access (E-UTRA); Physical Layer Procedures," 3GPP, Sophia Antipolis, Technical Specification 36.213 v.11.4.0, Sep. 2013.
[22] ——, "Spatial channel model for Multiple Input Multiple Output (MIMO) simulations," 3GPP, Sophia Antipolis, Technical Report 25.996 v.11.0.0, Sep. 2012.